Itinerant electron magnetism in $CaRu_{1-x}Mn_xO_3$ ($0 \leq x \leq 0.5$)

2009 J. Phys.: Condens. Matter 21 296002

(http://iopscience.iop.org/0953-8984/21/29/296002)

J. Phys.: Condens. Matter **21** (2009) 296002 (6pp) doi:10.1088/0953-8984/21/29/296002

Itinerant electron magnetism in $CaRu_{1-x}Mn_xO_3$ ($0 \leqslant x \leqslant 0.5$)

H Kawanaka[1], M Yokoyama[2], A Noguchi[2], H Bando[1] and Y Nishihara[2]

[1] National Institute of Advanced Industrial Science and Technology, Tsukuba, Ibaraki 305-8568, Japan
[2] Faculty of Science, Ibaraki University, Mito, Ibaraki 310-8512, Japan

Received 12 February 2009, in final form 5 June 2009
Published 3 July 2009
Online at stacks.iop.org/JPhysCM/21/296002

Abstract

The effect of Mn substitution in paramagnetic metal $CaRuO_3$ was studied by magnetization and neutron diffraction measurements. Development of ferromagnetic order is observed for $x \geqslant 0.2$ in $CaRu_{1-x}Mn_xO_3$. For the sample with $x = 0.4$, the Curie temperature of ~160 K is obtained from the Arrott plot and the ratio of effective moment and saturation moment $P_{\rm eff}/M(0)$ is estimated to be ~4.8. We further found that the magnetization is significantly suppressed with decreasing temperature T below ~90 K. In the neutron diffraction experiment at $T = 15$ K, we observed the evolution of a magnetic Bragg peak originating from the G-type antiferromagnetic order as well as the ferromagnetic one. This strongly suggests that both ferromagnetic and antiferromagnetic states are coexistent with each other at low temperatures. In the $M(T)_0^2$ against T^2 plot (here, $M(T)_0$ is a spontaneous magnetization estimated from the Arrott plot), $M(T)_0^2$ linearly increases with decreasing T^2 in the ferromagnetic region between ~90 and 160 K. The ferromagnetic properties of the $CaRu_{1-x}Mn_xO_3$ system ($x \leqslant 0.5$) are well explained in terms of spin fluctuation theory based on the itinerant electron model rather than the localized spin model.

1. Introduction

Ruthenium oxides are intensively studied because they show a rich variety of electronic and magnetic properties. $SrRuO_3$ is an itinerant electron ferromagnet with a Curie temperature of about 160 K and a saturation magnetic moment of 1.6 μ_B per Ru atom [1–4]. The conduction of $SrRuO_3$ is classified as an unconventional bad metal [4]. It is revealed that the substitution of Mn for Ru changes the electronic properties from a metallic ferromagnet to a semiconducting antiferromagnet [5–7]. Sr_2RuO_4 shows a unique superconductivity [8, 9] for which the spin-triplet pairing and multiphase structure of the superconductivity have been suggested from Ru-NMR, NQR, specific heat and thermal conductivity measurements. On the other hand, $CaRuO_3$ is believed to be a paramagnetic metal [10, 11], where the magnetization in high field shows typical paramagnetic behavior, while an irreversible temperature dependence of magnetization is observed in a low magnetic field [10]. It is reported [11] from the Ru-NMR study that the Stoner factor for $CaRuO_3$ is ~0.98 and the correlation factor in a modified Korringa relation is ~0.15. These results are evidence that the $CaRuO_3$ is a nearly ferromagnetic metal dominated by spin fluctuation with low frequencies and long-wavelength components.

Some of the previous reports [12–22] on substitution effects for $CaRuO_3$ point out that a ferromagnetic phase is significantly induced by the substitutions for both Ca and Ru, and thus suggest that a ferromagnetic instability is involved in $CaRuO_3$. More than 20% doping of Sr is found to evolve ferromagnetic order [12]. Many studies of the Ru-site substitution effects have been reported [13–22] and it is revealed that Ti, Fe, Ni and Mn substitutions also induce ferromagnetism. In the Ti doping system, though the ferromagnetic Curie temperature is nearly constant with Ti concentration, the magnetization shows a maximum around 30% doping of Ti [15]. Such a feature is considered to be due to an inhomogeneity of the ferromagnetic phase.

Transport and magnetic properties have been studied for Mn-rich concentrations in the Mn doping system [17–22]. The substitution of Ru for Mn in the antiferromagnetic insulator $CaMnO_3$ induces the ferromagnetism, and coincidentally the insulator–metal transition occurs [23]. In these papers the ferromagnetic order is explained by the double-exchange

mechanism between Mn^{3+} and Mn^{4+} ions and it is reported that the magnetic state is an inhomogeneous mixture of ferromagnetic and antiferromagnetic grains. However, the appearance of strong ferromagnetism is still observed for the Mn concentration less than 40% [21, 22]. Thus, we precisely studied magnetism in the Mn concentration region less than 50% by magnetization measurements and neutron diffraction experiments. Our experimental results strongly suggest that the ferromagnetism in the Ru-rich region is well explained in terms of the itinerant electron model rather than the inhomogeneous localized spin model. As far as we know, this is the first example of an itinerant electron ferromagnet following the spin fluctuation theory in mixed perovskite oxides. This system will supply valuable information for investigating magnetism at the boundary of localized and itinerant electrons. In this paper, we report the results of magnetization and neutron diffraction measurements in $CaRu_{1-x}Mn_xO_3$ system ($x \leqslant 0.5$) and analysis based on the spin fluctuation theory of the itinerant electron model [24–27].

2. Experimental procedure

The polycrystalline samples of $CaRu_{1-x}Mn_xO_3$ for $x = 0$, 0.1, 0.2, 0.3, 0.4 and 0.5 were prepared by the solid-state reaction method with starting materials of 4N purity $CaCO_3$, RuO_2 and MnO. The calcination was carried out at 740 °C for 4 h followed by sintering of the pelletized material at 1300 °C for 24 h. The samples were characterized by powder x-ray diffraction. The powder patterns for all the samples were in good agreement with the distorted perovskite structure with orthorhombic symmetry (the space group $Pnma$). The lattice parameters are $a = 5.506$ Å, $b = 7.681$ Å and $c = 5.369$ Å at RT for $x = 0$. No extra patterns due to other extrinsic phases were observed within the experimental accuracy. It is found that the lattice parameters decrease monotonically with increasing Mn concentration and reach $a = 5.407$ Å, $b = 7.607$ Å and $c = 5.341$ Å at $x = 0.5$.

Magnetization measurements were carried out using a SQUID magnetometer in fields up to 5 T and in the temperature range between 5 and 300 K. For resistivity measurements a conventional dc four-probe method was used. The neutron diffraction experiments for the powdered samples with $x = 0.4$ were performed on the Kinken powder diffractometer for high efficiency and high resolution measurements, HERMES, at the Institute for Materials Research (IMR), Tohoku University, installed at the JRR-3M reactor in the Japan Atomic Energy Agency (JAEA), Tokai. We used a neutron wavelength of 1.8265 Å.

3. Experimental results

Figure 1(a) shows the temperature dependence of magnetization $M(T)$ obtained under the field-cooled condition at an applied field H of 5 T. The $M(T)$ curves for $x = 0$ and 0.1 show weak temperature dependence. By the doping of Mn, on the other hand, the magnetization is enhanced and shows a strong temperature dependence. The value of magnetization for $x = 0.5$ is ten times as large as that for $x = 0$.

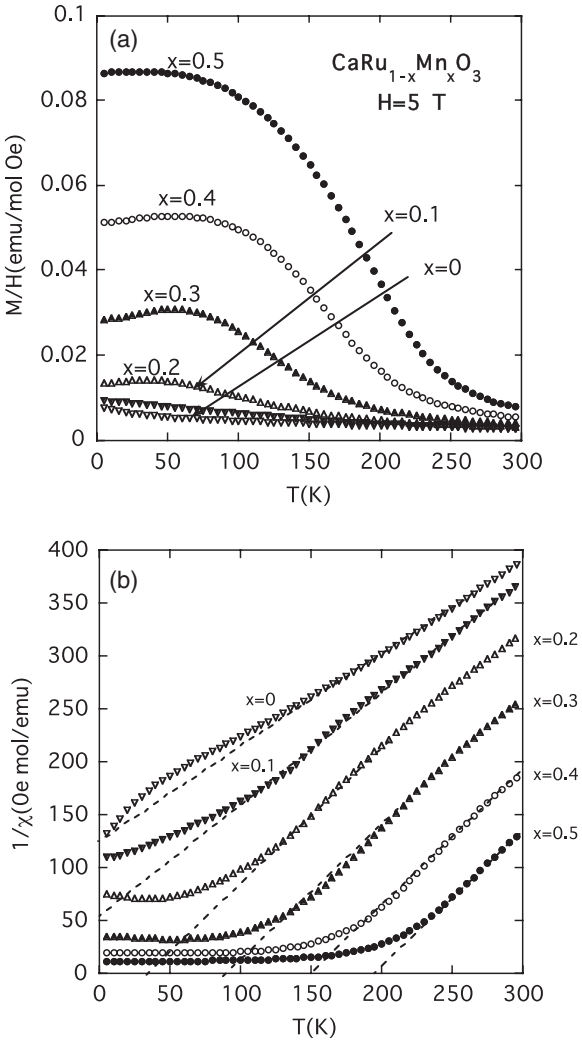

Figure 1. (a) Temperature dependence of molar susceptibility and (b) temperature dependence of inverse molar susceptibility at applied field H = 5 T for $CaRu_{1-x}Mn_xO_3$ ($0 \leqslant x \leqslant 0.5$). The Weiss constants in the text are determined from the Curie–Weiss law, indicated by dashed lines.

The temperature dependence of inverse susceptibility $1/\chi (=H/M)$ is shown in figure 1(b). In the high-temperature region the inverse susceptibility follows the Curie–Weiss formula $\chi(T) = C/(T - \theta)$. The Curie constant (C) and the Weiss constant (θ) were estimated from the linear part of the temperature dependence of $1/\chi$. The Curie constant is ∼0.9 for $x > 0.1$ which gives the effective moment of $\mu_{\rm eff} \sim 2.4\,\mu_{\rm B}$. while the Weiss constant monotonically increases from ∼20 K at $x = 0.1$ to ∼200 K at $x = 0.5$. This increase in the Weiss constant shows that the substitution of Mn for Ru induces ferromagnetism above $x = 0.2$.

The Arrott plot (M^2 versus H/M) for the ferromagnetic sample of $x = 0.4$ is shown in figure 2. We find that the M^2 shows a linear H/M dependence over a wide temperature and field range. The slope of these lines is nearly independent of temperature. It is well known that in the Arrott plot the magnetic transition temperature $T_{\rm C}$ is determined from the temperature where the interception of M^2 is zero. The obtained $T_{\rm C}$ is ∼160 K, which agrees well with the Weiss

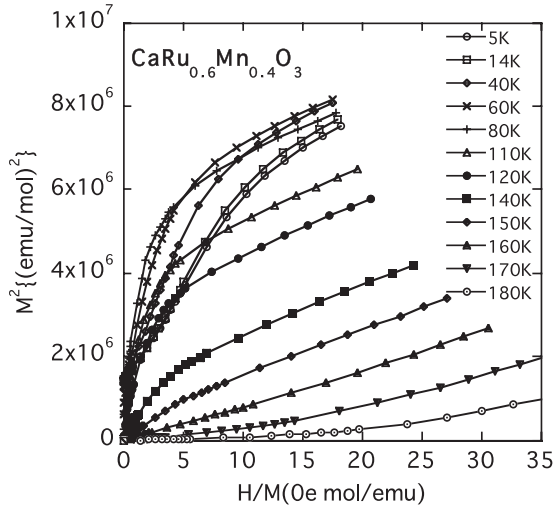

Figure 2. Arrott plot of magnetization for $CaRu_{0.6}Mn_{0.4}O_3$.

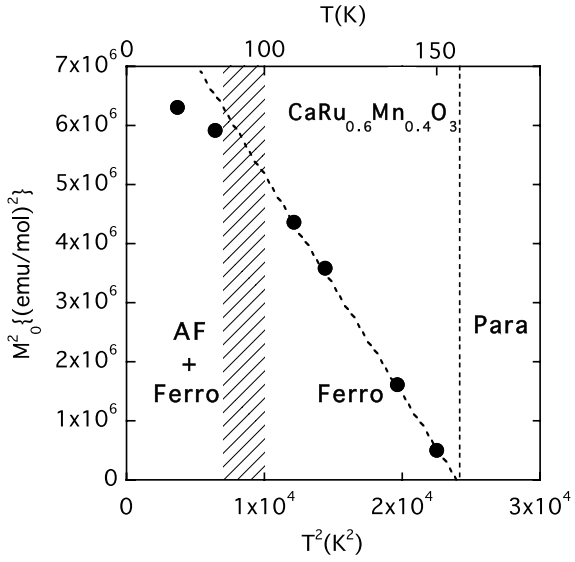

Figure 3. Square of spontaneous magnetization plotted against the square of temperature for $CaRu_{0.6}Mn_{0.4}O_3$.

constant ∼160 K obtained from the temperature dependence of $1/\chi$. In the very low field range, M^2 does not show the behavior of a ferromagnet. In addition, below 60 K the value of M^2 becomes smaller with decreasing temperature.

The square of spontaneous magnetization $M(T)_0^2$ at temperature T was obtained from the extrapolation of the linear part of the $M(T)^2$ curve to $H/M = 0$. Figure 3 shows the $M(T)_0^2$ against T^2 plot. The magnetization $M(T)_0^2$ linearly increases with decreasing T^2 below 160 K. Below ∼90 K, the $M(T)_0^2$ deviates from the linear relation. This is consistent with the result that the temperature dependence of magnetization shows a peak around 60 K, as is seen in figure 1. We can estimate the Curie temperature from the T^2 value at $M(T)_0^2 = 0$. This value gives the $T_C = 161$ K, agreeing well with the results of the Arrott plot.

From the linear part above 90 K we can estimate the saturation magnetization $M(0)$ at $T = 0$ K by extrapolation.

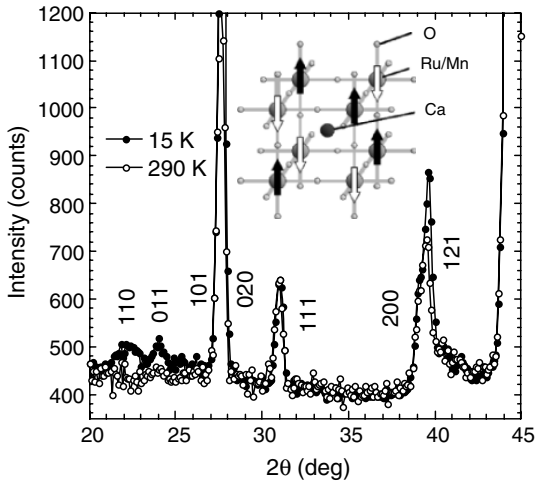

Figure 4. Neutron powder diffraction patterns at $T = 15$ K (closed circle) and 290 K (open circle) for $CaRu_{0.6}Mn_{0.4}O_3$. The enhancement of the (110) and (011) Bragg peak intensities at 15 K is due to the evolution of G-AF order, while that of the (121) peak intensity is ferromagnetic. The inset shows the spin arrangement on the Ru/Mn sites for the G-type AF structure, depicted in the unit cell of cubic perovskite structure.

The estimated value becomes $M(0) \sim 0.51\ \mu_B$. The itinerant feature of the itinerant magnet is usually evaluated by using the Rhodes–Wohlfarth ratio ($=P_c/M(0)$). The P_c is calculated from the experimental value of P_{eff} by $P_{eff} = [P_c(P_c + 2)]^{1/2}$. The ratio $P_c/M(0) \sim 3.2$ was obtained for this sample. The value is larger than 1. On the other hand, Takahashi [27] pointed out that the observed moment ratio $P_{eff}/M(0)$ is a good parameter for discussion of the itinerant nature of magnetic materials and a better universal relation than the Rhodes–Wohlfarth plot is obtained by the $P_{eff}/M(0)$ versus T_c/T_0 plot, where T_0 is a measure of the spectral width of spin fluctuation. The moment ratio of this sample is ∼4.8. In $SrRuO_3$ the moment ratio is estimated to be ∼2.2 [28]. The result suggests the itinerant character of this system is stronger than that of $SrRuO_3$.

We have observed the suppression of magnetization at low temperatures. To clarify its origin, we carried out neutron powder diffraction for $x = 0.4$. Our experimental results suggest that the G-type antiferromagnetic (G-AF) order evolves together with the ferromagnetic (F) one at low temperature. Figure 4 shows the neutron powder diffraction patterns at $T = 15$ K (closed circle) and 290 K (open circle). The intensities for the (200) and (121) peaks at 15 K are clearly larger than those at 290 K, and similar differences are detected for the other Bragg peak intensities. The difference of the peak intensity shows a tendency to decrease in the high-2θ region, indicating that they are mainly due to the ferromagnetic order. In addition, although the experimental error is fairly large, we observed the development of weak peaks at ∼22° and ∼24° in the low-temperature region. They are considered to correspond to the (110) and (011) Bragg peaks, respectively, which are expected to be enhanced by the AF ordering with the G-type modulation. These peaks are weak but clearly distinguished from the backgrounds below 90 K. The inset

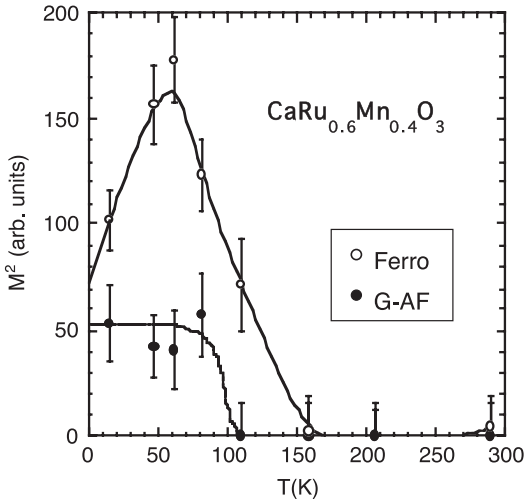

Figure 5. Temperature variation of the square of the volume-averaged magnetic moments for F (open circle) and G-AF (closed circle) orders.

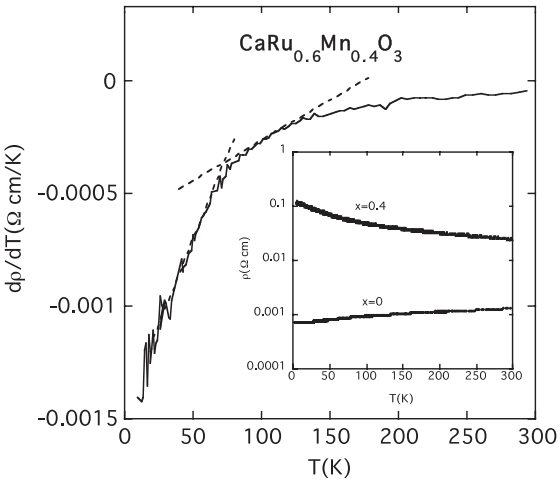

Figure 6. Temperature dependence of differential resistivity for $CaRu_{0.6}Mn_{0.4}O_3$. The inset shows the temperature dependence of resistivity for $x = 0.0$ and 0.4.

shows the spin arrangement on the Ru/Mn sites for the G-type AF structure, depicted in the unit cell of cubic perovskite structure for simplicity. The closed circles in figure 5 show the temperature variation of the square of the volume-averaged magnetic moments estimated from these peak intensities. In the present experimental accuracy, we cannot detect the other Bragg peak due to the corresponding structure at the high-2θ position. Nevertheless, we suggest that these Bragg peaks are ascribed to the occurrence of the G-AF order, because the same structure is also observed in the Mn-rich concentration range [17]. The intensities of magnetic Bragg peaks are reduced with increasing temperature. In figure 5 we plot the temperature variation of the square of the volume-averaged magnetic moments for F and G-AF orders, estimated from the integrated intensities of the magnetic Bragg peak intensities. The magnitude of the ferromagnetic moment increases below 150 K, and then shows a peak at ∼70 K followed by the suppression at low temperatures. Correspondingly, the G-AF structure evolves below ∼90 K. These properties are consistent with the characteristics seen in the Arrott plot, where the square of magnetization M^2 at very low fields and low temperatures does not follow the H/M linear dependence, and with the fact that the $M(T)_0^2$ deviates from the T^2 linear dependence below ∼90 K.

The temperature dependence of resistivity for $x = 0.4$ is shown in the inset of figure 6. The resistivity exhibits weakly semiconductive variation for all the temperature range. We could not observe a clear change in resistivity at the Curie temperature. In general the effect of magnetic scattering on resistivity is weak in itinerant electron systems. Figure 6 shows the temperature derivative of resistivity. The temperature dependence of the derivative kinks around ∼90 K and ∼150 K below which we observed the antiferromagnetic order and ferromagnetic order, respectively, by neutron diffraction.

4. Discussion

Our experimental results strongly suggest that the ferromagnetism in $CaRu_{1-x}Mn_xO_3$ ($x \leqslant 0.5$) is well explained in terms of the itinerant electron model rather than the localized one. In our magnetic measurements, the slope of the $1/\chi$ versus T plot in the ferromagnetic sample is nearly independent of the observed ferromagnetic moment. According to the spin fluctuation theory in the itinerant electron model, the Curie constant is independent of saturation moment at $T = 0$ K. It is rather determined from the ratio of the spectral width of the spin fluctuation and T_C [27]. Therefore, our experimental results agree well with the spin fluctuation theory of the itinerant electron model. The Curie–Weiss law holds even for paramagnetic metals near $CaRuO_3$, since they are very close to the ferromagnetic instability. In the localized electron model, the effective moment usually changes with Mn^{4+} doping and it is expected that the slope of the $1/\chi$ versus T plot also changes, which is in sharp contrast with our experiment results. These experimental results show that the $CaRuO_3$ is a nearly ferromagnetic metal dominated by the ferromagnetic spin fluctuation. However, the ferromagnetic interaction is not strong enough to induce ferromagnetism. This is the reason why the ferromagnetic order does not appear below $x = 0.2$.

In the itinerant electron model [26] the Curie constant is a reflection of the stiffness of the longitudinal spin fluctuation and the effective moment does not agree with that for the ionic model. In fact, the experimental value of effective moment is higher than the value estimated from the localized moment for the low spin state of the Ru^{4+} ion ($S = 1$). In the Arrott plot we observed the nearly constant slope behavior in wide temperature and field ranges. It will be very difficult to explain these features with the localized spin model.

In the Mn-rich region, it is suggested the origin of the ferromagnetism is the double-exchange interaction between Mn^{3+} and Mn^{4+} ions [23]. The moment ratios $P_{\rm eff}/M(0)$ in the typical double-exchange systems $La_{0.67}Ca_{0.33}MnO_3$ and $La_{0.67}Sr_{0.33}MnO_3$ are estimated to be ∼1.8 and ∼1.5,

Table 1. Curie temperature T_C, the saturation magnetization $M(0)$, the effective moment P_{eff} and the moment ratio $P_{eff}/M(0)$ in polycrystalline $CaRu_{0.6}Mn_{0.4}O_3$, $La_{0.67}Ca_{0.33}MnO_3$ and $La_{0.67}Sr_{0.33}MnO_3$.

	$CaRu_{0.6}Mn_{0.4}O_3$ (This work)	$La_{0.67}Ca_{0.33}MnO_3$ [29]	$La_{0.67}Sr_{0.33}MnO_3$ [29]
T_C (K)	161	270	376
$M(0)$ (μ_B)	0.51	3.39	3.59
P_{eff} (μ_B)	2.41	5.96	5.61
$P_{eff}/M(0)$	4.8	1.8	1.5

respectively [29], which are near the value estimated from the localized electron systems. However, our experimental value is ∼4.8, which is in the region estimated from the typical itinerant electron systems. Magnetic parameters of these samples are summarized in table 1. Therefore, the ferromagnetism in $CaRu_{1-x}Mn_xO_3$ system with low Mn concentrations should be explained by band magnetism rather than the ionic model.

In this system the $M(T)_0^2$ shows the T^2 dependence in the ferromagnetic region as shown in figure 3. The spin fluctuation theory of weak itinerant magnets predicts [24–27] that the squared spontaneous moment shows the T^2 dependence at low temperature as

$$(M(T)_0/M(0))^2 = 1 - (T/T_C)^2.$$

Around the critical temperature T_C it changes as follows:

$$M(T)_0^2 \propto T_c^{4/3} - T^{4/3}.$$

It is well known that the magnetization of the weak itinerant electron ferromagnet $ZrZn_2$ follows well the T^2 dependence [30]. This system also shows the T^2 dependence. In our temperature range the $T^{4/3}$ dependence was not observed.

We find that the magnetic state below ∼90 K is a coexistent state of ferromagnetic and antiferromagnetic states. Zeng *et al* [23] reported that the magnetic state is an inhomogeneous mixture of ferromagnetic and antiferromagnetic grains in the $CaRu_{1-x}Mn_xO_3$ system. However, our neutron diffraction experiment shows the ferromagnetic order appears below 150 K and the G-type antiferromagnetic order evolves below ∼90 K. Corresponding to the observed phase transitions, the temperature derivative of resistivity also shows kinks around ∼90 and ∼150 K. These results strongly suggest the uniform magnetic orders develop in this system. In itinerant electron systems, phase transitions between ferromagnetic and antiferromagnetic states are explained by the mode–mode coupling theory of spin fluctuations [26]. A coexistent state of ferromagnetic and antiferromagnetic states appears when the coupling between ferromagnetic and antiferromagnetic spin fluctuation is weak. It is clear from our experimental results that the ferromagnetic and antiferromagnetic spin fluctuations coexist in the $CaRu_{1-x}Mn_xO_3$ system.

Since the $CaMnO_3$ is a localized spin system, it is expected that d electrons have both itinerant and localized characters in the $CaRu_{1-x}Mn_xO_3$ system. The localized moment in the itinerant electron system may be formed as the moment in the virtual bound state [31, 32]. Though it is not clear at present that this type of virtual bound state is the origin of double-exchange ferromagnetism in Mn-rich regions, this system is suitable for studying the variation from the band to the localized magnetism.

5. Conclusions

In summary, the effect of Mn substitution in paramagnetic metal $CaRuO_3$ was studied by magnetization and neutron diffraction measurements. The evolution of ferromagnetic order is observed for $x \geqslant 0.2$ in $CaRu_{1-x}Mn_xO_3$. The magnetic susceptibility follows the Curie–Weiss law and the slope of $1/\chi$ versus T plot is nearly independent of the observed ferromagnetic moment. For the sample with $x = 0.4$, the M^2 shows a linear H/M dependence in wide temperature and field ranges. The square of spontaneous magnetization $M(T)_0^2$ at temperature T linearly increases with decreasing T^2 from 160 down to ∼90 K. The temperature and magnetic field dependences of magnetization are consistent with the spin fluctuation theory of the itinerant electron model. The Curie temperature of ∼160 K and the moment ratio $P_{eff}/M(0)$ of ∼4.8 were obtained from these results.

Below ∼90 K the value of magnetization becomes small with decreasing temperature. In the neutron diffraction experiment at $T = 15$ K, we observed evolution of the magnetic Bragg peak originating from the G-type antiferromagnetic order as well as the ferromagnetic one. The magnetic state below ∼90 K is a coexistent state of ferromagnetic and antiferromagnetic states, which is explained by the mode–mode coupling theory of spin fluctuations.

The ferromagnetic behavior in this system is well explained in terms of the spin fluctuation theory of the itinerant electron model rather than the localized spin model. The $CaRu_{1-x}Mn_xO_3$ system ($x \leqslant 0.5$) will be the first example of an itinerant electron ferromagnet following the spin fluctuation theory in mixed perovskite oxides.

Acknowledgment

We are grateful to K Ohoyama for technical support in the neutron diffraction experiments.

References

[1] Longo J M, Raccah P M and Goodenough J B 1968 *J. Appl. Phys.* **39** 1327
[2] Allen P B, Berger H, Chauvet O, Forro L, Jarlborg T, Junod A, Revaz B and Santi G 1996 *Phys. Rev.* B **53** 4393
[3] Kostic P, Okada Y, Collins N C, Schlesinger Z, Reiner J W, Klein L, Kapitulnik A, Geballe T H and Beasley M R 1998 *Phys. Rev. Lett.* **81** 2498
[4] Klein L, Dodge J S, Ahn C H, Snyder G J, Geballe T H, Beasley M R and Kapitulnik A 1996 *Phys. Rev. Lett.* **77** 2774
[5] Sahu R K, Hu Z, Rao M L, Manoharan S S, Schmidt T, Richter B, Knupfer M, Golden M, Fink J and Schneider C M 2002 *Phys. Rev.* B **66** 144415
[6] Yokoyama M, Satoh C, Saitou A, Kawanaka H, Bando H, Ohyama K and Nishihara Y 2005 *J. Phys. Soc. Japan* **74** 1706

[7] Cao G, Chikara S, Lin X N, Elhami E, Durairaj V and Schlottmann P 2005 *Phys. Rev.* B **71** 35104
[8] Maeno Y *et al* 1994 *Nature* **372** 532
[9] Ishida K *et al* 1998 *Nature* **396** 658
[10] Felner I, Nowik I, Bradaric I and Gospodinov M 2000 *Phys. Rev.* B **62** 11332
[11] Mukuda H, Ishida K, Kitaoka Y, Asayama K, Kanno R and Takano M 1999 *Phys. Rev.* B **60** 12279
[12] Cao G, McCall S, Shepard M, Crow J E and Guertin R P 1997 *Phys. Rev.* B **56** 321
[13] He T and Cava R J 2001 *Phys. Rev.* B **63** 172403
[14] He T and Cava R J 2001 *J. Phys.: Condens. Matter* **13** 8347
[15] Hardy V, Raveau B, Retoux R, Barrier N and Maignan A 2006 *Phys. Rev.* B **73** 94418
[16] Maignan A, Raveau B, Hardy V, Barrier N and Retoux R 2006 *Phys. Rev.* B **74** 024410
[17] Shames A I, Rozenberg E, Martin C, Maignan A, Raveau B, Andre G and Gorodetsky G 2004 *Phys. Rev.* B **70** 134433
[18] Markovich V, Fita I, Puzniak R, Martin C, Wisniewski A, Maignan A, Raveau B, Yuzhelevskii Y and Gorodetsky G 2004 *Phys. Rev.* B **70** 24403
[19] Hebert L, Pi S, Martin C, Maignan A and Raveau B 2003 *Phys. Rev.* B **67** 24430
[20] Markovich V, Auslender M, Fita I, Puzniak R, Martin C, Wisniewski A, Maignan A, Raveau B and Gorodetsky G 2006 *Phys. Rev.* B **73** 14416
[21] Maignan A, Martin C, Hervieu M and Raveau B 2001 *Solid State Commun.* **117** 377
[22] Taniguchi T, Mizusaki S, Okada N, Nagata Y, Lai S H, Lan M D, Hiraoka N, Itou M, Sakurai Y, Ozawa T C, Noro Y and Samata H 2008 *Phys. Rev.* B **77** 014406
[23] Zeng Z, Greenblatt M and Croft M 1999 *Phys. Rev.* B **59** 8784
[24] Moriya T and Kawabata A 1973 *J. Phys. Soc. Japan* **34** 639
[25] Moriya T and Kawabata A 1973 *J. Phys. Soc. Japan* **35** 669
[26] Moriya T 1985 *Spin Fluctuation in Itinerant Electron Magnetism* (Berlin: Springer)
[27] Takahashi Y 2001 *J. Phys.: Condens. Matter* **13** 6323
[28] Klein L, Dodge J S, Ahn C H, Reiner J W, Mieville L, Geballe T H, Beasley M R and Kapitulnik A 1996 *J. Phys.: Condens. Matter* **8** 10111
[29] Snyder G J, Hiskes R, DiCarolis S, Beasley M R and Geballe T H 1996 *Phys. Rev.* B **53** 14434
[30] Ogawa S 1968 *J. Phys. Soc. Japan* **25** 109
[31] Friedel J 1956 *Can. J. Phys.* **34** 1190
[32] Anderson P W 1961 *Phys. Rev.* **124** 41